NJC

Accepted Manuscript

This is an *Accepted Manuscript*, which has been through the Royal Society of Chemistry peer review process and has been accepted for publication.

Accepted Manuscripts are published online shortly after acceptance, before technical editing, formatting and proof reading. Using this free service, authors can make their results available to the community, in citable form, before we publish the edited article. We will replace this *Accepted Manuscript* with the edited and formatted *Advance Article* as soon as it is available.

You can find more information about *Accepted Manuscripts* in the Information for Authors.

Please note that technical editing may introduce minor changes to the text and/or graphics, which may alter content. The journal's standard Terms & Conditions and the Ethical guidelines still apply. In no event shall the Royal Society of Chemistry be held responsible for any errors or omissions in this *Accepted Manuscript* or any consequences arising from the use of any information it contains.

ROYAL SOCIETY OF CHEMISTRY

www.rsc.org/njc

New Sulfonated Poly (arylene ether sulfone)s Copolymers Containing Phenyl Side Chains as Proton Exchange Membranes

RiMing Chen[a], Guang Li[a] *

[a] State key laboratory for modification of chemical fibers and polymer materials, college of materials science and engineering, Donghua University Shanghai, PR China. rmc2005@yeah.net, *lig@dhu.edu.cn

Abstract

A new series of sulfonated poly(arylene ether sulfone) containing phenyl side groups with different sulfonation degree (SPAES-PQ-xx) were successfully synthesized through direct aromatic nucleophilic substitution polycondensation of 3,3'-disulfonate-4,4'-dichlorodiphenylsulfone, 4,4-dichlorodiphenylsulfone and phenylhydroquinon(PQ). The degree of sulfonation was realized by controlling quantities of the sulfonated monomer. The chemical and phase-separated structures of copolymers were characterized by proton nuclear magnetic resonance spectroscopy and atomic force microscopy. The properties of flexible and transparent SPAES membranes were evaluated. Compared to the hydroquinone-based SPAES membrane (SPAES-HQ-40), the effect of phenyl side group on water absorption, swelling properties and proton conductivity of SPAES-PQ-xx membranes were explored. The results demonstrated that introduction of phenyl side groups could keep better dimensional, thermal and oxidative stability compared with those of SPAES-HQ-40 membrane. In addition, the proton conductivity of SPAES-PQ-40 is up to 0.096 Scm^{-1} at 80 °C.

Keywords:

Proton exchange membrane, Poly (arylene ether sulfone)s, Phenyl, Stability

1. Introduction

Due to the increasing need for clean energy conversion systems, proton exchange membrane fuel cells (PEMFCs) are widely regarded as one kind of promising alternative power sources to the use of fossil fuels as energy generating systems[1]. The proton exchange membrane is a critical component in PEMFCs that acts as a separator for the reactants, a catalyst support, and provides ionic pathways for proton transport. State-of-the-art PEMs are made from perfluorinated sulfonic acid polymers (PFSA) utilized in current PEMFCs due to their excellent proton conductive properties, However, PFSA membranes typically show limitations such as high cost, high fuel crossover, and restricted temperature and humidity operating conditions which prevent a widespread use in PEMFCs[2]. These shortcomings have triggered an extensive worldwide search for alternative membrane materials with an improved property profile[3]. Many efforts have been made in order to enhance the properties of PEM containing hydrocarbon-based aromatic backbones. Polymers with desirable structure such as poly(phenylene)s[4, 5], poly(arylene ether ketone)s[6, 7], poly(arylene ether sulfone)s[8, 9], poly(arylene sulfide sulfone)s[10], poly(arylene ether)s[11, 12], and polyimides[13-15] have been investigated as potential PEM materials. Among these PEMs, sulfonated poly(arylene ether sulfone) (SPAES) is of considerable interest owing to its excellent thermal ability, mechanical strength, good longevity/stability under cell condition[16] and better oxidative stability [17, 18].

However, in comparison with PFAS membranes, aromatic statistical copolymer PEMs with the ionic sulfonic acid groups distributed along the backbone often have lower proton conductivity, which is largely related to their weaker acidity and poor hydrophilic and hydrophobic phase separation[19]. They reach high

New Journal of Chemistry Accepted Manuscript

proton conductivities at high ionic contents, which lead to high water uptake and loss dimensional stability. Herein, many efforts[20-24] have been made on chemical structure design of SPAES in hope of acquiring suitable morphological structure and balancing the performance for proton exchange membrane application. It is well known that critical membrane properties depend on both the molecular structure of the polymer and the phase separation between the hydrophobic polymer main chain segments provided the PEMs with mechanical strength and the sulfonated moieties responsible for proton conductivity[25, 26]. Byungchan et al. reported that the smaller hydrophobic components, such as planar naphthylene groups, induced larger and more developed hydrophilic clusters, whereas larger ones such as isopropylidene bis(biphenylene) caused smaller and dispersed hydrophilic domains. The small hydrophobic components induced high proton conductivities and proton diffusion coefficients as well as low water swelling, and were also favorable for low gas permeability and high mechanical strength[27].

Inspired by this earlier research, we introduced a phenyl group as small hydrophobic component into sulfonated poly (arylene ether sulfone) side chains, which has possibility to improve oxidative stability as well as dimensional stability. Among fuel cell related properties, we primarily focus on water uptake, dimensional stability, proton conductivity, oxidative stability and phase-separated structures of SPAES-PQ-40 in comparisons with SPAES-HQ-40. Finally, these properties related to PEM are discussed with aspects of molecular design and application of future polymer electrolytes in mind.

2. Experimental

2.1 Materials

Highly purified, commercially available 4,4'-dichlor-odiphenylsulfone (DCDPS), 3,3'-disulfonate-4,4'-dichlorodiphenylsulfone (SDCDPS) was obtained from shanghai darui finechemical Company. Phenylhydroquinon monomer was prepared from 1'4-benzoquinone and aniline, and it was synthesized by the same method as we have previously reported[28]. Hydroquinone-based disulfonated poly(arylene ether sulfone) copolymer(SPAES-HQ-40) was gained from Yan Jin Technology Co., Ltd. Anhydrous potassium carbonate, toluene, and N,N-dimethylacetamide (DMAc) were purchased from Aldrich and used as received. All the other chemicals and solvents were reagent grade and used without further purification unless otherwise noted.

2.2 Measurement

^{1}HMR spectra were recorded on Bruker AV 400 MHz, using deuterated dimethyl sulfoxide (DMSO-d6) as solvent and tetramethylsilane(TMS) as internal standard. Inherent viscosities (η_{inh}) were measured at a concentration of 0.5 g/dL in DMAc at 25 °C with an Ubbelohde viscometer. Differential scanning calorimetry (DSC) analysis was performed on a TA Q20 DSC instrument at a heating rate of 20 °C/min from 50 °C to 350 °C in a nitrogen atmosphere. Thermogravimetric analysis (TGA) was employed to assess the thermal stability of the membranes, using a TA Discovery thermal system. Before measurement, the membrane sample pieces were dried. The samples were equilibrated to 50 °C and then heated to 800 °C at 20 °C /min in a nitrogen atmosphere. The temperatures at 5% (Td5) and 10% (Td10) weight loss were recorded for each sample.

The composite morphology was evaluated using an atomic force microscope (AFM).Tapping mode AFM

New Journal of Chemistry Accepted Manuscript

was performed with a Digital Instrument Agilent 5500, using micro-fabricated cantilevers with a force constant of approximately 40 N/m. All samples were dried at 60 °C for 24 h under vacuum conditions. The samples were imaged immediately in ambient conditions.

The mechanical properties were assessed on an Instron 5969 tensile apparatus with a 5 kg load cell at a crosshead speed of 5 mm/min. The dumbbell-shaped specimen is approximately 40–60 μm thick and 4 mm gauge wide with a 50 mm gauge length. Five individual specimens were used for each sample.

2.3 Preparation of SPAES-PQ-xx polymers

As shown in scheme 1, the SPAES-PQ-40 was prepared by direct polymerization. Sulfonated monomer SDCDPS 0.9924g 2mmol), unsulfonated monomer DCDPS (0.8745g 3mmol), isphenol onomer phenylhydroquinon (0.9502g 5mmol), 10 mmol (1.382 g) anhydrous potassium carbonate, 15 mL DMAc, and 15 mL toluene were added to a 100 mL three-necked flask equipped with a magnetic stirrer, a condenser, a Dean-Stark trap, and a nitrogen inlet. The reaction mixture was heated under reflux at 160 °C for 6 h, which stripped off most of the toluene to dehydrate the system. Then the temperature was raised slowly to 190 °C and maintained until the solution became viscous, after which it was precipitated into 500 mL ethanol with vigorous stirring, then filtered. The resultant was washed thoroughly with hot water and dried at 120 °C under vacuum for 48 h.

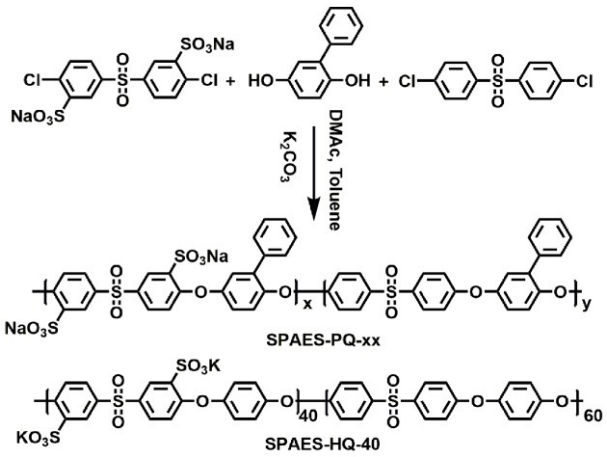

Scheme 1 Synthesis of SPAES-PQ-xx and the chemical structure of SPAES-HQ-40 polymers

2.4 Preparation of SPAES membranes

First, the salt form of the random polymer (0.6g) was dissolved in DMAc (15 mL) with stirring at room temperature for 12 h. Then, the solution was filtered using a funnel and cast onto glass dishes (diameter 90 mm). The thickness of all membranes was in the range of 50-80 μm. After careful drying at 60 °C for 48 h under vacuum, smooth and flexible membranes were obtained. The resulting membranes were immersed in 1M H_2SO_4 solution at room temperature for 48 h to permit the exchange of Na^+ with H^+. Finally, the membranes were soaked and washed thoroughly with deionized water to remove excessive H_2SO_4 and stored in deionized water for testing.

2.5 Ion exchange capacity, water uptake and swelling ratio

The ion exchange capacity (IEC, meq g^{-1}) of the sulfonated polymer membranes was determined using a typical titration method. Square pieces (10 mm × 30 mm) of the membranes in acid form were soaked in 20

New Journal of Chemistry Accepted Manuscript

mL of a 1 M NaCl solution and equilibrated for at least 48 h to replace the protons with sodium ions. The H^+ ions released from the membranes were then titrated with a 0.1 M NaOH solution using phenolphthalein as an indicator. The IEC was defined as mequiv of sulfonic groups per gram of dried sample, via the following formula:

$$IEC\ (meq\ g^{-1}) = (V_{NaOH} \times C_{NaOH})/W_{dry} \quad (1)$$

where V_{NaOH} is the consumed volume of NaOH, C_{NaOH} is the molar concentration of NaOH, and W_{dry} is the weight of dried membrane.

The IEC values, which were calculated from the sulfonation degree (DS), were obtained from the following equation[29]:

$$IEC = 1000DS/(M+80DS) \quad (2)$$

Where, DS is the degree of sulfonation and calculated from the ^{1}H-NMR. M is the molecular weight of the polymer structure unit not containing sulfonic acid.

The swelling of the membranes (10 mm × 30 mm) was evaluated by their water uptake (WU), which was estimated from the mass change before and after the membrane completely dry. A dry membrane was submerged in deionized water in a fully hermetic flask at controlled temperatures for a day, then the surface water was wiped off carefully with filter paper, and the membrane was immediately weighed. Before the testing, the sample was dried in a vacuum oven at 80 °C for 48 h, the WU was calculated using the equation:

$$\text{Water uptake} = (W_{wet} - W_{dry})/W_{dry} \times 100\% \quad (3)$$

where W_{wet} and W_{dry} are the masses of the fully hydrated membrane and the dry membrane, respectively.

The swelling ratio was measured to evaluate the membrane dimensional stability. The membrane samples (10 mm × 30 mm) were vacuum dried at 80 °C for 48 h, then were immersed in deionized water at a constant temperature for a day. After the surface water carefully wiped off, the length (Lx) and width (Ly) of the membrane samples were quickly measured. Thus, the swelling ratio (SR) of each membrane was calculated using the expressions:

$$S = L_x \times L_y$$

$$SR = (S_{wet} - S_{dry})/S_{dry} \quad (4)$$

where S_{wet} and S_{dry} are the area of the fully hydrated membrane and of the dry membrane, respectively.

2.6 Proton conductivity

Prior to the measurement, the membrane was immersed in 1M H_2SO_4 at room temperature for 48 h and then washed to a pH of 7 with deionized water. After kept in deionized water over 48 h. The proton conductivity of the SPAES membranes (8 mm × 10 mm) was measured by an AC impedance technique using an electrochemical impedance analyzer (VMP2/Z, PAR), whereby the AC frequency was scanned from 100 kHz to 1 Hz at a voltage amplitude of 100 mV. Fully hydrated membrane was sandwiched in a Teflon@ conductivity cell equipped with Pt foil contacts[30]. The membrane was in contact with water throughout the measurement. The impedance was tested by placing the cell in a temperature-controlled chamber. The proton conductivity was calculated from the following equation:

$$\sigma = L/RA \quad (5)$$

where L and A are the thickness and the contact area of the membrane sample, respectively, and R is the

New Journal of Chemistry Accepted Manuscript

membrane resistance.

2.7 Oxidative stability

Square pieces of the membrane samples (10 mm × 30 mm) were immersed in Fenton's reagent (3% H_2O_2 containing 2 ppm $FeSO_4$) at 80 °C. The oxidative stability was evaluated by recording the retained weights of the membranes after treatment in Fenton's reagent for 1 h, and the time when the membranes wholly disappeared.

3 Results and discussion

3.1 Synthesis of SPAES-PQ-xx polymers

The SPAES-PQ-xx polymers were successfully prepared via modified nucleophilic aromatic substitution polycondensation of phenylhydroquinon, DCDPS and SDCDPS, with DMAc as the solvent, which contained toluene as a dehydration agent. The DS of the polymers were simply controlled by varying the ratio of SDCDPS to DCDPS. Table 1 lists the SPAES polymers and membranes prepared in this study, along with inherent viscosities. The chemical structures of the gained SPAES polymers were identified by ^{1}H-NMR, which has often been used to determine the structure and DS values of sulfonated polymers [31, 32]. These high intrinsic viscosities indicate that all the polymers exhibit high molecular weight and can be cast into flexible and tough membranes. The viscosity is direct proportional to the feed ratio of SDCDPS, we believe that the amount of strong polar sulfonic groups has affected on viscosity. As shown in Fig.1, the aromatic protons of H3 located at the orthoposition of sulfonic acid groups displayed a higher frequency (8.24-8.29 ppm) due to the deshielding effect of the sulfonic acid groups. The presence of each -SO_3H group resulted in distinct signals for protons at the H3 positions. The intensity of the H3 signals was used to estimate their content, which was equivalent to the content of -SO_3H groups per average repeat unit of copolymer. As a result, the desired sulfonated copolymers were obtained.

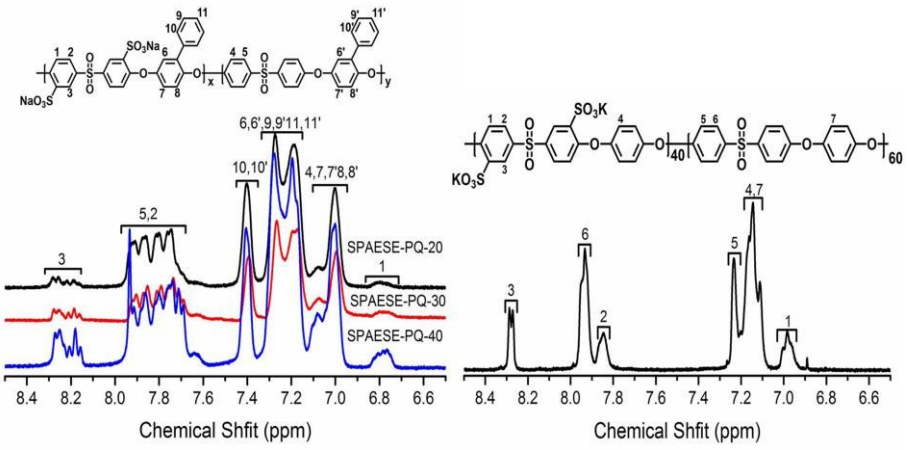

Fig. 1 ^{1}H-NMR spectra of SPAES-PQ-xx and SPAES-HQ-40 polymers

As seen in Table 1, the IEC, an indicator of a polymer membrane's capacity to exchange ions, is closely related to proton conductivity, and thus has a major effect on membrane performance. IEC values, which were calculated from the ^{1}H-NMR spectra of the SPAES samples are presented from 0.82-2.02 mequivg^{-1}, are coincided with the titration ones. The IEC from the titration test were in the range of 0.84-1.96 mequivg^{-1}. These mean that the sulfonic acid groups were successfully attached to the polymer backbone by polycondensation.

New Journal of Chemistry Accepted Manuscript

Table 1 SPAES polymers prepared and their membranes properties.

Membrane	SDCDPS/ DCDPS	η_{inh} (dLg^{-1})[a]	DS(%) from ^{1}H-NMR	IEC (meq g^{-1}) ^{1}H-NMR	IEC (meq g^{-1}) titration
SPAES-PQ-20	2/8	1.31	32	0.82	0.84
SPAES-PQ-30	3/7	1.12	52	1.17	1.21
SPAES-PQ-40	4/6	0.98	74	1.61	1.56
SPAES-HQ-40	4/6	0.8	78	2.02	1.96

[a] The polymers in acid form was measured at a concentration of 0.5 g/dL in DMAc at 25 °C.

3.2 Thermal and mechanical properties of SPAES membranes

The thermal property of SPAES membranes in acid form were investigated by DSC and TGA. The results are presented in Figs. 2 (a) and (b). The Fig. 2(a) shows the DSC curves of the SPAES membranes. For the SPAES membranes, the Tg increased to 213 °C for SPAES-PQ-30 and further increased to 251 °C for SPAES-PQ-40. This can be explained by the increased intermolecular interaction and molecular bulkiness arising from the sulfonic acid groups, both of which factors hindered internal rotation in the SPAES polymers[33]. However, the Tg values of SPAES-HQ-40 is 112 °C from the DSC curves. The absence of Tg is probably due to the fact that no bulky pendant groups to hinder intermolecular interactions and movement of molecular segments and strengthen the regularity of molecular chain. As shown in Table 2, the Tg values of the SPAES-PQ-xx are all above 200 °C which further suggests the excellent thermal properties of the SPAES-PQ-xx presented in this work. When the temperature of operating PEMFCs is around 100 °C, which is so far below that of Tg values. Thus, the SPAES-PQ-xx membranes show good thermal stability.

TGA curves of the membranes were recorded from 50 °C to 800 °C, under a nitrogen flow at a heating rate of 20 °C min^{-1} to assess their short-term thermal stability. From the TGA curves (Fig. 2(b)), all of the SPAES membranes studied in this work also displayed two typically and major weight loss stages[34] at around 200-450 °C and 460-600 °C which is ascribed to the removal of -SO_3H groups and the splitting of the polymer main chain. The slight weight loss under 150 °C of all the samples can be explained by the expulsion of water molecules from the polymer matrix or of moisture absorbed from the air**.** Especially, the SPAES-PQ-20 had higher weight loss temperature. Moreover, the 5% weight loss temperature of SPAES-PQ-xx decreased with increasing sulfonation degree. These phenomena are because the first weight loss of SPAES-PQ-xx results from desulfonation, similar to other sulfonated polymers[35]. The 10% weight loss temperature of SPAES-PQ-xx was higher than that of SPAES-HQ-40. This may be attributed to phenyl pendant is in favor for promoting chain entanglement and enlarges the rigid of the backbone to enhance the thermal properties of SPAES-PQ-xx.

New Journal of Chemistry Accepted Manuscript

Table 2 The thermal properties of SPAES membranes

Polymer Membrane	Tg (°C)[a]	Td5 (°C)[b]	Td10 (°C)[c]
SPAES-PQ-20	209	530	553
SPAES-PQ-30	213	474	520
SPAES-PQ-40	251	324	496
SPAES-HQ-40	112	247	301

[a] The second trace of DSC measurements conducted at a heating rate of 20 °C min^{-1} in nitrogen.

[b] Temperature at which 5% weight loss was observed.

[c] Temperature at which 10% weight loss was observed.

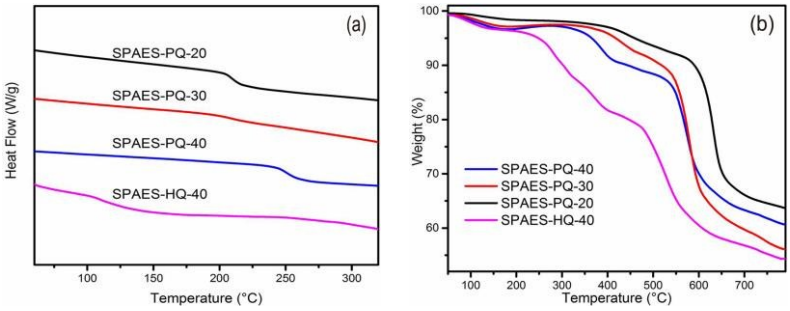

Fig. 2 DSC (a) and TG (b) curves of SPAES membranes

In addition to thermal properties, robust mechanical properties are essential for the fabrication of membrane electrode assembly for fuel cell applications. The mechanical properties of the SPAES membranes were determined at room temperature and in wet. These results were listed in Table 3. It is interesting to observe that the tensile strengths of all the tested SPAES membrane samples are in the range of 21.55-32.11 MPa, with modulus values in the range of 0.57-1.01 GPa. The ensile strength and modulus of the SPAES-PQ-xx membranes were higher than for SPAES-HQ-40. The elongation at break of the SPAES-PQ-xx membrane ranged from 3.70% to 19.40%, whereas SPAES-HQ-40 has a higher elongation at break. The phenyl pendant group is in favor for promoting chain entanglement and enlarges the rigid of the backbone.

Table 3 The mechanical properties of SPAES membranes

Polymer Membrane	Tensile strength (MPa)[a]	Tensile modulus (GPa) [a]	Elongation at break (%) [a]
SPAES-PQ-20	32.11	0.61	3.70
SPAES-PQ-30	23.54	1.01	19.40
SPAES-PQ-40	22.65	0.89	12.12
SPAES-HQ-40	21.55	0.57	83.13

[a] The samples were measured in the hydrous states at room temperature.

3.3 Water uptake and swelling ratio

Water is the main vehicle by which protons are transported through the membrane. Therefore, desired water content is an essential requirement for promoting proton conductivity. However, excessively high levels of water in the membrane can result in excessive dimensional changes (swelling) leading to failures in mechanical properties. The dimensional stability is a crucial property for PEMs in membrane electrode

New Journal of Chemistry Accepted Manuscript

assembly[36]. Fig. 3(a) shows the water uptake of the SPAES-HQ-40 and SPAES-PQ-xx membranes at different temperatures. It can be seen that the water uptake of all the membranes increased with DS and temperature, and the SPAES-HQ-40 membrane exhibited a much higher water uptake than the others. Compared to the membranes with lower DS values, the membrane with a high DS value had a higher free volume due to the strong hydrophilicity of the -SO_3H groups. Moreover, as Fig. 3(c) shown, the values of λ[37] (the number of H_2O molecules per sulfonic acid group) were obtained for all the membranes. The λ values of SPAES membranes increased with the temperature. The λ value of SPAES-HQ-40 was much higher than that of SPAES-PQ-xx from 30 °C to 80 °C. The higher water uptake of SPAES-HQ-40 membrane could be expected to be beneficial for proton transport. These are consistent with SPAES-HQ-40 membrane having best proton conductivity among them.

In Fig. 3(b), the swelling ratios (SR) for the SPAES membranes are provided to evaluate the membranes dimensional stability. The SR of the SPAES-PQ-xx membranes increased with DS and temperature, as it had in the case of water uptake. For SPAES-HQ-40, the membrane showed a higher SR than SPAESE-PQ-40 from 30 °C to 80 °C. However, the SR was nearly 2-fold that of SPAES-PQ-40 membranes at 80 °C. These results suggest that SPAES-PQ-40 membranes possess good dimensional stability, especially in hot water. SPAES-HQ-40 thus suffer excessive swelling because of the almost perfoliate hydrated ionic domains, similar to the previous reports[24]. The above results demonstrate that the introduction of phenyl could depress its water uptake and enhanced the dimensional stability.

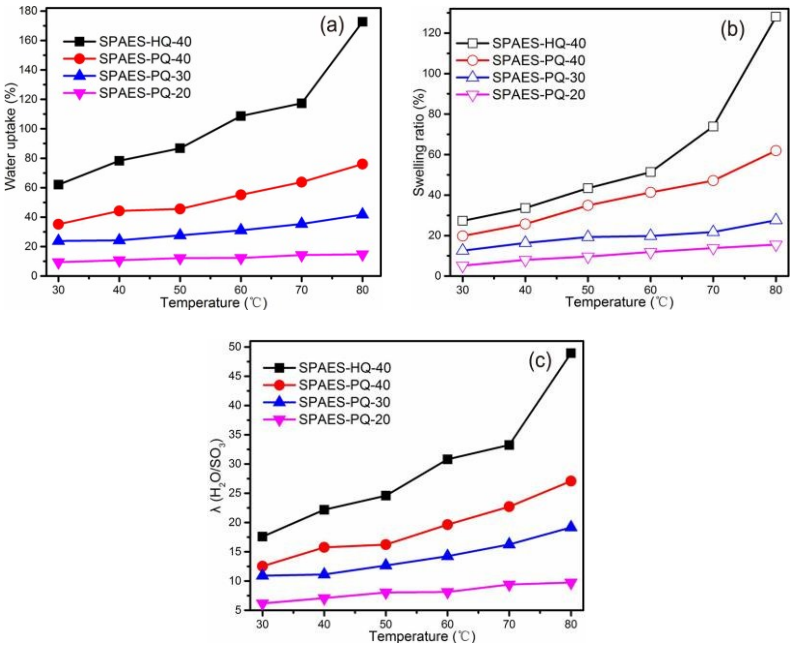

Fig. 3 Temperature dependence of water uptake (a), swelling ratio (b) and hydration number λ (c) for SPAES membranes

New Journal of Chemistry Accepted Manuscript

3.4 Oxidative stability

Proton exchange membranes are known to undergo degradation resulting from hydroxyl or peroxyl free radicals formed by the decomposition of H_2O_2 generated at cathode during operational conditions of fuel cells[17]. To evaluate whether the membranes could withstand a stronger oxidizing environment during fuel cell operation, the oxidative stability of SPEAS membranes were investigated by immersing the films (10 mm × 30 mm) into Fenton's reagent (2 ppm $FeSO_4$ in 3% H_2O_2) at 80 °C. Their oxidative stability were evaluated by measuring their retained weights after treatment in Fenton's reagent for 1 h at 80 °C, and at the time when the membranes wholly disappeared. As can be seen in Table 4, the oxidative stability of SPAESE-PQ-xx membranes decreased with increasing DS. The retained weight of these SPAES-PQ-xx membranes after treatment in Fenton's reagent for 1 h was close to or even higher than that of SPAES-HQ-40. The time required for the SPAES-PQ-40 membranes to dissolve in Fenton's reagent completely was longer than for SPAES-HQ-40. Such a stability enhancement should benefit from phenyl side chains, where the proton was confined in hydrophilic domains and the polymer backbone can be well protected by the additional hydrophobic structure.

Table 4 Oxidative stability and △Ea of SPAES-HQ-40 and SPAES-PQ-xx membranes

Polymers	Oxidative stability		△Ea (kJmol^{-1})
	RW (%)[a]	t (h)[b]	
SPAES-PQ-20	96.89	140.5	13.92
SPAES-PQ-30	93.38	128.0	12.20
SPAES-PQ-40	95.31	3.5	11.97
SPAES-HQ-40	91.63	2.0	10.89

[a] Retained weights of membranes after treatment in Fenton's reagent for 1 h at 80 °C.

[b] The dissolving time of the polymer membrane.

3.5 Proton conductivity

The proton conductivities of the fully hydrated SPAES-HQ-40 and SPAES-PQ-xx membranes were estimated using AC impedance diagrams, and the results at different temperatures are displayed in Fig. 4(a). All the tested membrane samples showed proton conductivities that increased with DS and temperature. Such conductivity behavior could be attributed to the increased IEC based on sulfonic acid groups (Table 1) and the improved water uptake at elevated temperature (Fig. 3). That is, both the high mobility of free ions and a number of charge carriers are effective in the present conducting system. For SPAES-HQ-40, the proton conductivity even outperformed SPAES-PQ-40 .This can be explained by the Arrhenius formula[38]:

$$\ln\sigma - \ln\sigma_o = \triangle Ea/RT \qquad (6)$$

where σ is proton conductivity (Scm^{-1}), σ_o is the pre-exponential factor, △Ea is the apparent activation energy of proton transportation (kJmol^{-1}) and reflects the degree of influence that temperature has on proton conductivity, R is the thermodynamic constant (8.314 Jmol^{-1}K^{-1}), and T is the absolute temperature

New Journal of Chemistry Accepted Manuscript

(K). Linear regression of natural lnσ vs. 1/T was performed assuming an Arrhenius relationship, as presented in Fig.4 (b). The ion-transport activation energy values for SPAES membranes, derived from the slopes of the Arrhenius plots, are in the range of 10.89-13.92 kJ mol^{-1}. As Table 4 shows that the △Ea values are all higher than what would occur in a general aqueous system (around 10 $kJmol^{-1}$), it is deduced that proton transport mainly occurs via a vehicle-type mechanism, whereby the water molecules act as the active sites of H^+ transport via hydrogen bonding[39].

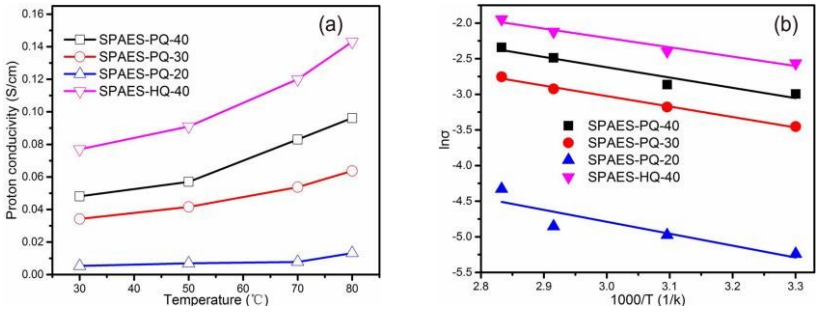

Fig. 4 (a) Proton conductivity and (b) Arrhenius plots of proton conductivity of SPAES membranes at various temperatures (in wet)

3.6 Phase morphology of SPAES membranes

The microstructure of PEM greatly affects their macroscopic properties such as water uptake, swelling and proton conductivity[40]. For comparison purpose, the morphologies of SPAES-PQ-40 and SPAES-HQ-40 membranes were examined by using AFM under tapping mode. The AFM height and phase images were recorded on a 500 nm × 500 nm size scale under ambient conditions as given in Fig 5 (A), (a) and (B), (b). As shown, their morphologies were shown by the bright and dark regions. Generally, the bright regions are composed of the hydrophobic backbone, endowing the membranes with mechanical strength, while the dark domains are formed by the hydrophilic sulfonic acid groups containing some amount of absorbed water, responsible for proton transport[41]. As Fig 5 (a) and (b) showed, the AFM phase images of SPAES-HQ-40 and SPAES-PQ-40 are apparent. However, the proton-hydrophilic-rich regions of SPAES-HQ-40 membranes are more distributed over non-ionic matrix and much more connective ionic domains compared with those of the SPAES-PQ-40 membranes. These different morphologies are a key to explain the dependence of proton conductivity between SPAES-HQ-40 and SPAES-PQ-40 membranes. For the SPAES-HQ-40 membrane, the presence of hydrophilic regions arrangement is relatively flexible, that is, it is easy to change the shape and size of domains. This feature enables the connections of network of conductive paths when the water content increase[42]. The SPAES-PQ-40 membrane with bulky phenyl side chain increased the rigidity and size of hydrophobic segments, and decreased the mobility of hydrophilic segments. This is the reason that why SPAES-HQ-40 showed higher proton conductivity, water uptake and swelling than that of SPAES-PQ-40.

New Journal of Chemistry Accepted Manuscript

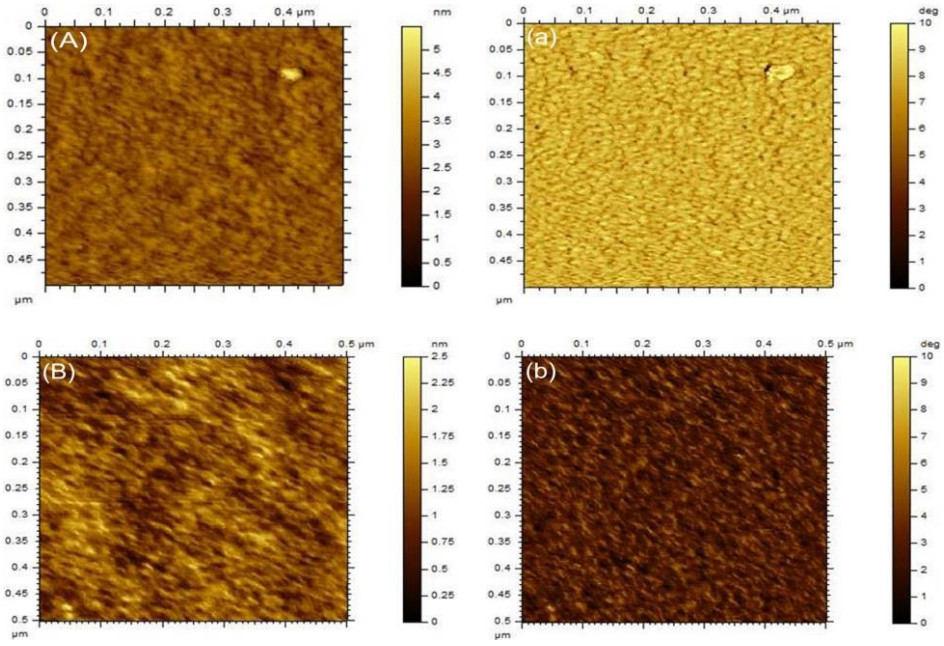

Fig. 5 AFM images of SPAES-PQ-40, SPAES-HQ-40. (A)–(B) are height images, (a)–(b) are phase images.

4 Conclusions

In short, a series of novel sulfonated poly(arylene ether sulfone) containing phenyl side chains with different sulfonation degree (SPAES-PQ-xx) were prepared by direct polymerization. The sulfonation degree ranged from 40% to 80% was controlled by changing the feed ratio of 3,3'-disulfonate-4,4'-dichlorodiphenylsulfone to 4,4-dichlorodiphenylsulfone. The membranes cast from solution displayed tensile strength of 22.65-32.11 MPa and had good thermal stability. The proton conductivity of SPAES-PQ-xx membranes were greatly improved by increasing both the sulfonation degree and the temperature. The proton conductivity of SPAES-PQ-40 achieved 0.096 Scm^{-1} at 80 °C. Compared with hydroquinone-based disulfonated poly(arylene ether sulfone), the SPAES-PQ-40 membrane exhibited better oxidative stability, thermal stability and dimensional stability. The results show that incorporation of phenyl side chains into the SPAES polymer markedly increased dimensional stability and raised oxidative stability. It concluded that small hydrophobic component with rigid side improve chains thermal and oxidative stability, but sacrifice the proton conductivity.

Acknowledgments

This work was financially supported by the Graduate Degree Thesis Innovation Foundation of Donghua University（grant 15D310618. the financial support is gratefully acknowledged.）

References

1. G. J. K. Acres, *Journal of Power Sources*, 2001, **100**, 60-66.
2. M. P. Rodgers, L. J. Bonville, H. R. Kunz, D. K. Slattery and J. M. Fenton, *Chemical Reviews*, 2012, **112**, 6075-6103.

New Journal of Chemistry Accepted Manuscript

3. Y. Gao, G. P. Robertson, M. D. Guiver, G. Wang, X. Jian, S. D. Mikhailenko, X. Li and S. Kaliaguine, *Journal of membrane science*, 2006, **278**, 26-34.
4. S. Seesukphronrarak and A. Ohira, *Chemical communications*, 2009, 4744-4746.
5. T. Kobayashi, M. Rikukawa, K. Sanui and N. Ogata, *Solid State Ionics*, 1998, **106**, 219-225.
6. B. Liu, G. P. Robertson, D.-S. Kim, M. D. Guiver, W. Hu and Z. Jiang, *Macromolecules*, 2007, **40**, 1934-1944.
7. L. Fu, G. Xiao and D. Yan, *Journal of Membrane Science*, 2010, **362**, 509-516.
8. P. Jannasch, *Fuel Cells*, 2005, **5**, 248-260.
9. B. Lafitte and P. Jannasch, *Advanced Functional Materials*, 2007, **17**, 2823-2834.
10. K. B. Wiles, F. Wang and J. E. McGrath, *Journal of Polymer Science Part A: Polymer Chemistry*, 2005, **43**, 2964-2976.
11. F. Wang, M. Hickner, Q. Ji, W. Harrison, J. Mecham, T. A. Zawodzinski and J. E. McGrath, *Macromolecular Symposia*, 2001, **175**, 387-396.
12. K. Miyatake and A. S. Hay, *Journal of Polymer Science Part A: Polymer Chemistry*, 2001, **39**, 3211-3217.
13. K. Miyatake, H. Zhou and M. Watanabe, *Macromolecules*, 2004, **37**, 4956-4960.
14. J. Fang, X. Guo, S. Harada, T. Watari, K. Tanaka, H. Kita and K.-i. Okamoto, *Macromolecules*, 2002, **35**, 9022-9028.
15. J. Saito, K. Miyatake and M. Watanabe, *Macromolecules*, 2008, **41**, 2415-2420.
16. W. Harrison, M. Hickner, Y. Kim and J. McGrath, *Fuel cells*, 2005, **5**, 201-212.
17. J. Lawrence and T. Yamaguchi, *Journal of Membrane Science*, 2008, **325**, 633-640.
18. J. Lawrence, K. Yamashita and T. Yamaguchi, *Journal of Power Sources*, 2015, **279**, 48-54.
19. K.-D. Kreuer, S. J. Paddison, E. Spohr and M. Schuster, *Chemical Reviews*, 2004, **104**, 4637-4678.
20. T. J. Peckham and S. Holdcroft, *Advanced materials*, 2010, **22**, 4667-4690.
21. Y. S. Kim, B. Einsla, M. Sankir, W. Harrison and B. S. Pivovar, *Polymer*, 2006, **47**, 4026-4035.
22. T. J. Peckham, J. Schmeisser, M. Rodgers and S. Holdcroft, *Journal of Materials Chemistry*, 2007, **17**, 3255-3268.
23. Q. Li, Y. Chen, J. R. Rowlett, J. E. McGrath, N. H. Mack and Y. S. Kim, *ACS Applied Materials & Interfaces*, 2014, **6**, 5779-5788.
24. A. Roy, M. A. Hickner, B. R. Einsla, W. L. Harrison and J. E. McGrath, *Journal of Polymer Science Part A: Polymer Chemistry*, 2009, **47**, 384-391.
25. K. Miyatake, K. Oyaizu, E. Tsuchida and A. S. Hay, *Macromolecules*, 2001, **34**, 2065-2071.
26. S. J. Wang, J. J. Luo, M. Xiao, D. M. Han, P. K. Shen and Y. Z. Meng, *International Journal of Hydrogen Energy*, 2012, **37**, 4545-4552.
27. B. Bae, K. Miyatake and M. Watanabe, *Macromolecules*, 2009, **42**, 1873-1880.
28. J. Xie, W.-y. Peng, G. Li and J.-m. Jiang, *Polymer bulletin*, 2011, **67**, 45-56.
29. N. Zhang, J. Li, X. Wang, Z. Xia and H. Liu, *Journal of Applied Polymer Science*, 2009, **114**, 304-312.
30. J. Qiao, J. Fu, L. Liu, J. Zhang, J. Xie and G. Li, *Solid State Ionics*, 2012, **214**, 6-12.
31. Y. Gao, G. P. Robertson, M. D. Guiver, S. D. Mikhailenko, X. Li and S. Kaliaguine, *Macromolecules*, 2004, **37**, 6748-6754.
32. S. J. Zaidi, S. Mikhailenko, G. Robertson, M. Guiver and S. Kaliaguine, *Journal of Membrane Science*, 2000, **173**, 17-34.

New Journal of Chemistry Accepted Manuscript

33. F. Wang, M. Hickner, Y. S. Kim, T. A. Zawodzinski and J. E. McGrath, *Journal of Membrane Science*, 2002, **197**, 231-242.
34. R. Nolte, K. Ledjeff, M. Bauer and R. Mülhaupt, *Journal of Membrane Science*, 1993, **83**, 211-220.
35. L. Fu, G. Xiao and D. Yan, *ACS Appl Mater Interfaces*, 2010, **2**, 1601-1607.
36. A. Roy, M. A. Hickner, O. Lane and J. McGrath, *Journal of Power Sources*, 2009, **191**, 550-554.
37. N. Li, S. Y. Lee, Y.-L. Liu, Y. M. Lee and M. D. Guiver, *Energy & Environmental Science*, 2012, **5**, 5346.
38. N. Li, D. W. Shin, D. S. Hwang, Y. M. Lee and M. D. Guiver, *Macromolecules*, 2010, **43**, 9810-9820.
39. J. Qiao, T. Hamaya and T. Okada, *Chemistry of materials*, 2005, **17**, 2413-2421.
40. K. Kreuer, *Journal of membrane science*, 2001, **185**, 29-39.
41. Y. S. Kim, M. A. Hickner, L. Dong, B. S. Pivovar and J. E. McGrath, *Journal of Membrane Science*, 2004, **243**, 317-326.
42. N. Takimoto, L. Wu, A. Ohira, Y. Takeoka and M. Rikukawa, *Polymer*, 2009, **50**, 534-540.

New Journal of Chemistry Accepted Manuscript

Table of Contents:

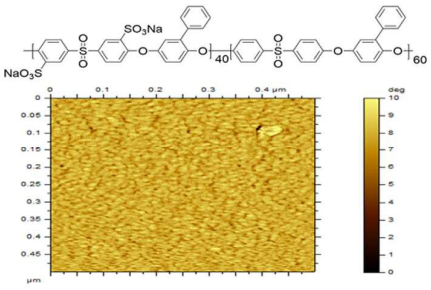

The chemical structure and phase images of SPAES-PQ-40 membrane

New Journal of Chemistry Accepted Manuscript